J. Soil Sci. and Agric. Eng., Mansoura Univ., Vol. 6 (10): 1217 - 1236, 2015

THERMAL PERFORMANCE ANALYSIS FOR SOLAR COLLECTOR AIR HEATER ASSISTED SOLAR MODIFIED-QUONSET DRYER

Abdellatif, S. M.; Y. M. El-Hadidi; and Eman M. Y. Mohammed
Dept. of Agricultural Engineering, Faculty of Agric. Mansoura University

ABSTRACT

This paper presents an experimental analysis to study and test the thermal performance of a novel mixed mode solar dryer (modified-quonset form) with solar collector air heater that could be used to dry seedless grape. The solar dryer consists of a flat-plate solar collector and a solar dryer. The thermal performance analysis tests were carried out on the roof of Agricultural Engineering Department (latitude angle of 31.045ºN, longitude angle of 31.37ºE, and altitude of 14.5 m above the sea level) during summer season of 2015 (from 29/8/2015 to 3/9/2015). The thermal performance analysis of the mixed mode solar dryer (forced convection system) based on the energy balance equations was evaluated. The solar dryer with forced convection was operated under mass flow rate of 0.1172 kg/s (6.58 m^3/min). The obtained data showed that, the daily average solar radiation recorded on the horizontal surface during the experimental period was 5.607 kWh/m^2 whilst, the actual solar radiation recorded on the tilted surface of flat-plate solar collector was 8.109 kWh/m^2. Consequently, the stationary non-tracking flat-plate solar collector increased the actual received solar radiation during that period by 44.62%. The daily averages solar radiation recorded outside and inside the solar dryer, respectively, were 5.607 and 4.570 kWh/m^2 with cover effective transmittance of 81.51%. The daily averages solar energy available inside the flat-plate solar collector and the solar dryer were 16.217 and 9.141 kWh of which 10.895 and 5.514 kWh, respectively, converted into useful heat gain. These solar energy available inside the flat-plate solar collector and the solar dryer resulting in increasing the indoor air temperatures above the outdoor (31.1°C) by 10.5, and 16.1°C, and reduce the air relative humidity under the outside (60.8%) by 28.3%. The daily average overall thermal efficiencies of the flat-plate solar collector and the solar tunnel dryer during the drying period were 66.64% and 59.52%, consequently, 33.36% and 40.48% of the solar energy available were lost, respectively.

Keywords: flat-plate solar collector, solar dryer, modified quonset form; thermal performance analysis tests.

INTRODUCTION

Solar energy is a kind of clean and freely available renewable energy that can simply be utilized for different heating applications upon conversion into thermal energy by using flat-plate solar air heaters. Because of, their simplicity, cheapness, and little maintenance requirements, flat-plate solar collectors in the system for the utilization of solar thermal energy are widely used in various equipment. They are namely used for solar energy collection, storage, and application. Collection of both beam and diffuse solar radiation are another advantage of flat-plate solar collectors. A conventional solar air collector generally consists of an absorber black plate with a parallel plate

below forming a small passage through which the air is to be heated and flows (Sukhatme and Nayak, 2008).However, the overall thermal efficiency of the flat-plate solar air heaters are relatively low, as the low heat transfer coefficient between the absorber plate and the air passing through lead to a higher temperature on the absorber plate, resulting in a higher rate of heat energy loss to the convection environment (Goel and Vashishtha, 2010; Kumar et al., 2014). Another reason for the low thermal performance of solar air heaters is the heat loss through the top cover (glazing), as all sides and bottom of the solar collector are thermally insulated (Nowzari et al., 2015).

Various studies have been carried out in order to increase the overall thermal performance of the solar collectors by modifying the configuration of the absorber plate. Making a cross-corrugated absorber plate (Lin, et al., 2006), locating porous material inside the solar collector instead of the solid metallic sheet (Tian et al., 2004), and adding fins to the black absorber plate (El-khawajah et al., 2011). An absorber black plate was constructed with fins and baffles by Yeh et al. (2000), to create turbulent flow and extend the heat transfer area per unit area of the absorber plate and investigated their effect on the overall thermal efficiency. The obtained results revealed that the baffled solar air heater had better thermal efficiency as compared with conventional solar air heaters. A cross-corrugated solar air collector with two wave-like plates was studied and tested by Lin et al. (2006). They concluded that a higher thermal efficiency can be achieved at higher air mass flow rates. Mittal and Vershney (2006) studied and tested optimal thermo-hydraulic performance of a wire mesh packed solar air heater. The resulting values of effective thermal efficiency indicated higher useful heat gain with the packed-bed collectors than with the smooth solar collectors. Cordeau and Barrington (2011) tested and examined an unglazed solar air pre-heater consisting of a perforated corrugated siding and found that the thermal efficiency of the unglazed solar air heater dependent upon the wind speed.

Several solar energy drying systems have been designed, constructed and utilized as alternative techniques to the traditional open-sun drying system, particularly in areas having a maximum possible of sunshine hours. According to the previous studies and researches these solar dryer systems can be classified in three forms as direct, indirect, and mixed modes, depending upon the arrangement of system components and mode of solar heat energy utilization (Afriyie et al., 2009; Chen and Qu, 2014). Greenhouse dryer system comes in the category of the direct solar drying system and also sometimes mixed mode drying system. The applicability of greenhouses is limited due to high indoor air temperature during hoter months of the year (Condori and Saravia, 2003). An experimental analysis to study and investigate the thermal performance of a novel mixed mode solar greenhouse dryer with forced convection for drying red pepper and sultana grape was executed by Elkhadraoui et al. (2015). They revealed that the drying rate in the solar greenhouse dryer could be much higher than that for the traditional open sun drying. Therefore, the drying time of red pepper and grape by novel mixed mode solar greenhouse dryer, respectively, was 17 and 50 h, whilst, the moisture content of red pepper was reduced to 16%(wb) within 24 h and the moisture content of sultana grape was reduced to 18% (wb) in 76 h.

The main objective of this research work was to; develop a low-cost flat plate solar collector air heater capable of moderate air temperature rises that can be connected to a modified-quonset solar dryer to constitute a novel mixed mode of forced convection solar dryer for drying seedless grape and other applications required hot air in a short time period, and test the thermal performance of the system.

MATERIALS AND METHODS

A solar collector air heater was designed and constructed in the workshop of the Agricultural Engineering Department, and installed on the roof of the Agricultural Engineering Department at Mansoura University (latitude angle 31.045ºN, longitude angle 31.37ºE and 14.5 m mean altitude above the sea level). The geometrical characteristics of the solar collector are of; total length 2.0 m, total width 1.0 m, depth 0.10 m, net surface area 2.0 m^2 as revealed in Fig. (1). It consisted of four basic components; collector casing, absorber plate, insulator, and glass cover. The collector casing is rectangular in shape, and made of aluminium bar 25 mm thick. The gross dimensions of the collector casing are 2.10 m long, 1.10 m wide and 0.11 m deep, with a net upper surface area of 2.31 m^2. A 50 mm of packed rock-glass wool insulator with thermal conductivity of 0.040 W/m ºC is placed in the bottom and sides of the collector casing to reduce the heat losses from the sides and back of the collector casing.

A corrugated absorber plate is formed of thin copper sheet 0.8 mm thick which is an excellent conductor of heat. Corrugation technique was used to increase the absorption surface area of the absorber plate per unit area of solar collector. It is painted with matt black paint to absorb the maximum possible amount of solar radiation flux incident on it. To reduce the reflection of solar radiation and reduce heat loss by convection, a clear glass cover 5 mm thick is placed to cover the collector casing. The air space between the corrugated absorber plate and the clear glass cover is 50 mm as suggested by ASHRAE (2005). The solar air heater was orientated toward the equator (stationary non-tracking) and inclined at 21.8º to the horizontal plane. This tilt angle was computed according to the following equation (Duffie and Beckman, 2006):

β= Latitude angle (Φ) - declination angle (δ) (1)

The solar air heater is connected to the solar tunnel dryer by one junction consisted of two different materials, 2.0 m long of plastic hoes-pipe and 2.0 m of galvanized water pipe (2-inch diameter). The ambient air is passed through the solar collector air heater along a corrugated absorber black plate at which it may be heated above the ambient air temperature. After the air passes through the solar collector air heater, it is entered into the solar dryer. The heated air was upward penetrated the grapes in the dryer tray. Therefore, the drying air was continuously introduced from the bottom and leaves through the top as shown in Fig. (2). One volumetric flow rate of air drying 5.86 m^3/min (0.1172 kg/s) was used for solar tunnel dryer during the experimental work.

Forced Convection Solar Dryer

A modified-quonset form solar dryer was designed and constructed in the workshop of the Agricultural Engineering Department, and installed on the roof of the department at Mansoura University. The experimental solar dryer having geometric characteristics of; total length 2.00 m, total width 1.00 m, vertical wall height 0.70 m, curved end height 0.31 m, length of arc 1.40 m, eaves height 1.01 m, floor surface area 2.0 m^2, and volume 1.813 m^3, as shown in Fig. (3) and Fig. (4). The solar dryer structural frame is formed of 12.7 mm galvanized water pipes. It also having an air chamber with gross dimensions of 2.0 m long, 1.0 m wide, and 0.30 m deep made of galvanized steel sheet with a net drying surface area of 2.0 m^2. The western top curved end of the solar tunnel dryer is connected to a blower (0.5-hp electric motor power at speed of 3000 rpm, and 220 V) by an air duct of 10.2 cm (4-inch) in diameter.

Fig. (1): Solar air heater used as an assisted system for solar dryer

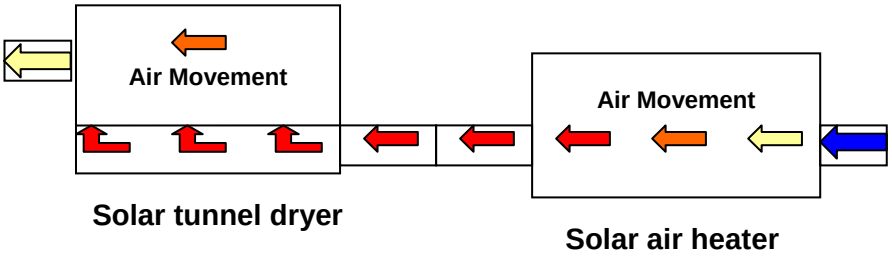

Fig. (2): Dying air movement through the solar collector air heater and the solar tunnel dryer during the experimental period.

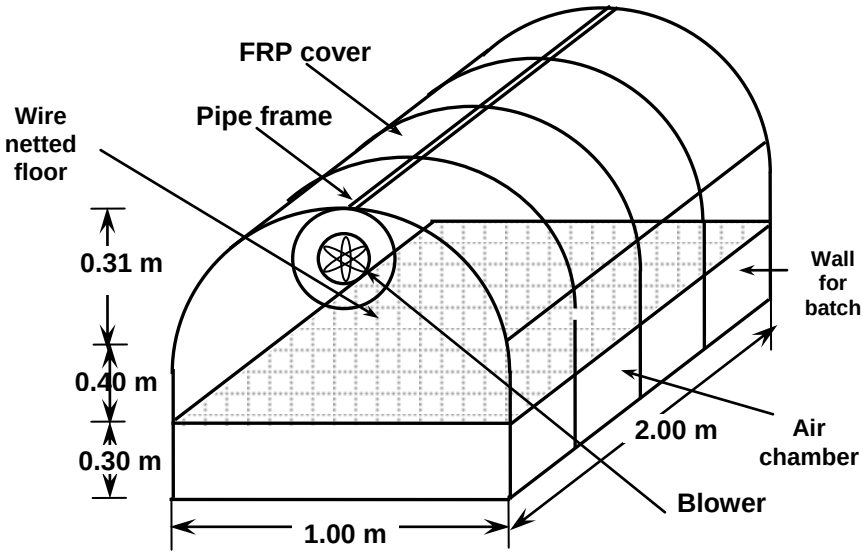

Fig. (3): Schematic diagram of the active solar dryer.

Fig. (4): Solar dryer (Modified-quonset form) for drying seedless grape.

The air drying was controlled by a controller air valve to provide the desired level of mass flow rate required for drying seedless grapes. The eastern bottom section (air chamber) is connected to an air duct of 5.08 cm (2-inch) for interring the hot drying air heated by individual solar collector air heater. The solar tunnel dryer is supported by four legs (25 cm high). The solar tunnel dryer is covered with single layer of flat fiberglass reinforced plastic (FRP) 1000µm thick. To increase and maintain the durability of structural frame and fiberglass cover, four tensile galvanized wires (2.0 mm

diameter) coated by plastic layer were tied and fixed throughout the longitudinal curved and vertical surface. It was orientated in East-West direction, where the southern longitudinal direction faced into the sun's rays.

Instruments and Data Acquisition

During the experimental work, several measurements were executed using different measuring devices.

Meteorological data

Meteorological station (Vantage Pro 2, Davis, USA) located in the Station of Agricultural Experiments and Researches Faculty of Agriculture Mansoura University (far away about 500 m from the location of this experimental work) was used to provide measures of different macroclimate variables such as, the solar radiation flux incident on a horizontal surface (pyranometer), dry-bulb, wet-bulb, and dew-point air temperatures (ventilated thermistor), wind speed and its direction (cup anemometer and wind vane), and air relative humidity (hygrometer). It also includes a small solar panel to power the wireless weather station during the daylight and charges the super capacitor for night operation. Lithium battery provides backup at nighttime. These sensors are connected to a data-logger system in order to test, display, and record the data during the experimental period. Data displayed on the video screen and updated by a scan of all the sensors every 60 seconds. The means of 5 scans are recorded on hard-disk every 5 minutes using software run to transfer the data automatically each day during the research work.

Air temperature and relative humidity

Microclimate variables within the centre of solar dryer were measured using data-logger (Watch-dog, 1000 series, USA). These microclimate variables included the solar radiation flux incident inside the solar dryer, dry-bulb air drying temperature, and air relative humidity. The air temperature just leaving the solar collector air heater, drying air temperature in the middle section of the drying chamber, and the drying air temperature just leaving the solar dryer was measured using 12 channel data-logger (Digi-sense scanning thermometer type) for taking and storing reading data from different sensors (thermocouple type K). The velocity of exhaust drying air was measured using a digital hot wire thermometer with measuring range from 0.1 to 10 m/s and accuracy of ± 0.1m/s.

Methods

Experimental procedure and data analysis

The experimental work was carried out during summer season of 2015(from 29/8 to 3/9/2015). A solar collector air heater assisted solar tunnel dryer was functioned to analysis the thermal performance of both systems.

Thermal performance analysis of solar air heater (solar collector)

The basic parameter to consider is the solar collector overall thermal efficiency. This is defined as the ratio of the useful heat energy delivered to the solar energy flux incident on the collector aperture. Under steady-state conditions, the thermal performance analysis can be measured and determined using the system analysis of Kalogirou (2004); ASHREA (2005); and Duffie and Beckman (2006) as follows:

Solar energy available (q)

The solar energy available was computed using the following equation:

$$q = R\ A_c, \quad \text{Watt} \qquad (2)$$

Where, R, is the solar radiation flux incident on the tilted surface of the solar collector in W m^{-2}, and, A_c, is the surface area of the solar collector in m^2.

Absorbed solar radiation (q_a)

The absorbed solar energy can be calculated from the solar energy available and the optical efficiency from the following formula:

$$q_a = R\ A_c\ (\tau\ \alpha), \quad \text{Watt} \qquad (3)$$

Where, τ α, is the optical efficiency of the solar collector in decimal, τ, is the effective transmittance of glass cover in decimal, and, α, is the effective absorptance of the absorber plate in decimal. The transmittance of glass cove and the absorptivity of the absorber black plate can be computed by the following equations:

$\tau = \tau_{max.} - 0.00437 \exp [0.0936 (\theta - 30)]$

$\alpha = \alpha_{max.} - 0.00476 \exp [0.040 (\theta - 35)]$

θ = solar incident angle on the tilted surface, degree

$\theta = \arccos (\cos \Psi \cos \gamma_{ss} \sin \beta + \sin \Psi \cos \beta)$

Ψ = solar altitude angle, degree

$\Psi = \arcsin (\sin \Phi \sin \delta + \cos \Phi \cos \delta \cos \omega)$

γ_{ss} = solar-surface azimuth angle, degree

$\gamma_{ss} = \gamma_s = \text{arcsen} [(\cos \delta \sin \omega)/\cos \Psi]$

The solar collector is orientated to face the equator and tilted from the horizontal with an inclined angle of 21.8º (stationary non-tracking) in such a way that they will minimize the angle of incidence and maximize the transmittance of glass cover and absorptance of the absorber plate at and around noon only. Consequently, the effective transmittance of glass cover (τ) and the effective absorptance (α) of the absorber plate, varied from sunrise to sunset and reached to the maximum values at noon (0.9 and 0.95, respectively) Therefore, the optical efficiency (τ α) of the solar collector will be at the maximum value of 0.855 at noon.

Useful heat gain (q_u)

The maximum possible useful energy gain (heat transfer) in a solar collector occurs when the whole collector is at the inlet fluid (air) temperature, heat losses to the surroundings are then at minimum. The useful heat gain can be calculated using the following formula:

$$q_u = m\ C_p\ (T_{aic} - T_{aoc}), \quad \text{Watt} \qquad (4)$$

Where, m, is the mass flow rate of air in kg s^{-1}, C_p, is the specific heat of air in J kg^{-1} $^oC^{-1}$, T_{aic}, is the inlet air temperature of solar collector in ºC, and, T_{aoc}, is the outlet air temperature of solar collector in ºC.

Solar collector heat losses (q_L)

The solar collector heat losses can be defined as the difference between the absorbed solar energy and the useful heat gain.

$$q_L = q_a - q_u, \quad \text{Watt} \qquad (5)$$

But several researchers (ASHRAE, 2005; Duffie and Beckman, 2006) reported that, the solar collector heat losses can be found from the following equation:

$$q_L = A_c\ U_o\ (\overline{T}_p - T_a)\ , \qquad \text{Watt} \qquad (6)$$

Where, $\overline{T}_p$, is the mean temperature of the absorber plate in °C, T_a, is the ambient air temperature in °C.

Overall thermal efficiency (η_o)

Solar collector overall thermal efficiency depends strongly upon the useful heat gain to storage and the energy collected by the panel. The solar panel overall thermal efficiency can be found from the following equation:-

$$\eta_o = \frac{q_u}{q} \times 100 = \frac{q_u}{A_c\ R} \times 100\ , \% \qquad (7)$$

Normalized temperature rise (D_T)

Normalized temperature rise of the solar collector is the difference between the outlet air and inlet air temperatures per solar radiation flux incident. It can be computed from the following relation:

$$D_T = \frac{T_{aoc} - T_{aic}}{R}\ , \text{m}^2\ ^\circ\text{C W}^{-1} \qquad (8)$$

Thermal performance analysis of the solar dryer (modified-quonset)

For many solar dryer systems, air is an ideal operating fluid which can be used to remove moisture from agricultural products. Heat energy added and removed from this type of solar dryer unit by transport the operating fluid (air), thus eliminating the temperature drop between transport fluid and drying chamber. The typical system in which air tank (solar tunnel dryer as a perfectly stirred tank) is used, can be represented by the solar air heating system. The heat energy balance on the solar dryer can be computed as follows (ASHRAE, 2005; Duffie and Beckman, 2006):

$$Q = Q_u + Q_{loss}, \qquad \text{Watt} \qquad (9)$$

The solar energy available inside the solar tunnel dryer (Q) can be computed as a function of solar radiation penetrated the tunnel cover and the net surface area of dryer as follows:

$$Q = R_i\ A_d, \qquad \text{Watt} \qquad (10)$$

Where, R_i, is the solar radiation flux incident on the horizontal surface inside the solar dryer in W m^{-2}, and, A_d, is the interior surface area of the solar tunnel dryer in m^2.

The useful heat gain by the solar tunnel dryer can be expressed as follows:

$$Q_u = m\ C_P\ (T_{aid} - T_{aod}), \qquad \text{Watt} \qquad (11)$$

Where, T_{aid}, is the inlet air temperature of solar tunnel dryer in ºC, and, T_{aod}, is the outlet air temperature of solar tunnel dryer in ºC.

The overall thermal efficiency (η_{od}) of the solar tunnel dryer, defined as the ratio of useful heat gain over any time period to the incident solar radiation over the same period.

$$\eta_{od} = \frac{Q_u}{R\ A_d} \times 100\ ,\ \% \qquad (12)$$

The total thermal losses from the inside solar dryer to the surrounding environment by conduction and convection, air exchange, and thermal radiation can be calculated from the following equation:

$$Q_{loss} = q_c + q_e + q_r\ ,\quad \text{Watt} \qquad (13)$$

The thermal losses by conduction and convection from the solar tunnel dryer can be assessed by limiting the heat transfer to conduction and convection, when the overall heat transfer coefficient (U_o, in W m^{-2} $^oC^{-1}$), total surface area of the solar tunnel cover (A_{cd}) in m^2, and the air temperature difference between average inside (T_{avi}) and ambient air outside (T_a) in ^oC are known or measured. The procedure does not require the separation of the conduction and convection components. It can be calculated from the following formula:

$$q_c = U_o\ A_{cd}\ (T_{avi} - T_a),\quad \text{Watt} \qquad (14)$$

The heat energy loss by forced air exchange (q_e) can be computed by assessing the rate of extracting fan discharge (V) in $m^3\ s^{-1}$, density of drying air (ρ) in kg m^{-3}, specific heat of air at constant pressure (C_P) in J kg^{-1} $^oC^{-1}$, and temperature difference between the average air inside (T_{avi}) and air just leaving the solar tunnel dryer (T_{aod}) in ^oC, as follows:

$$q_e = V\ \rho\ C_p\ (T_{avi} - T_{aod})\ ,\quad \text{Watt} \qquad (15)$$

The heat energy loss by thermal radiation (q_r) can be calculated in terms of the mean emittance factor of the inside solar dryer (ε), average transmissivity coefficient for long-wave radiation (τ) in decimal, *Stefan-Boltzmann* constant (σ) in W m^{-2} K^{-4}, floor surface area of the dryer (A_d) and absolute temperature difference between average inside air and the sky (T_{sky}) in ^oK, as follows:

$$q_r = \varepsilon\ \tau\ \sigma\ A_d\ (T_{avi}^4 - T_{sky}^4)\ ,\quad \text{Watt} \qquad (16)$$

$$T_{sky} = 0.0552\ (T_a)^{1.5}\ ,\ ^oK \qquad (17)$$

The thermal performance analysis tests for the flat plate solar collector and solar tunnel dryer using the previous equations were computed using Excel program. The obtained data from the experimental work were statistically analyzed using also Excel program. Linear regression analysis was functioned to test the relationship between the characteristics of the drying air and the drying rate. Multiple regression analysis was also used to correlate the drying rate with moisture content of grapes, drying air temperature, air relative humidity, and air mass flow rate. Significance level of 0.05 was conventionally taken as the minimum level of significance. Though where higher levels of significance were found these values were included in the text ($P \leq 0.01$ and $P \leq 0.001$).

RESULTS AND DISCUSSION

The flat-plate solar collector air heater and solar dryer have been operated satisfactorily for approximately six days without any malfunction. For the duration of the experimental work there were 78 hours of bright sunshine of which 54 hours (69.23%) were recorded and used in the thermal performance analysis. Air was continually cycled through the solar collector in clear sky conditions. After passing through the solar collector, the heated air was entered into the solar tunnel dryer. The operating fluid (air) flow rate was adjusted and controlled using an air control valve located at the outlet point of the flat plate solar collector. Under clear sky conditions, the solar energy available (q), absorbed solar energy (qa), useful heat gain (q_u), and overall thermal efficiency (η_o) increased gradually with solar time from sunrise until they attained the maximum values at noon. They then declined until reached the minimum values prior to sunset. The thermal performance analysis of the flat-plate solar collector is mainly measured by its overall thermal efficiency in converting solar radiation into solar thermal energy. The obtained data during the experimental period are summarizing and listed in Table (1).

Table (1): Hourly average solar energy flux incident on the tilted surface (R), solar energy available (q) and solar energy absorbed (q_a), useful heat gain (q_u), heat energy losses (q_L), and overall thermal efficiency during the experimental period.

Solar Time, hr	R, W/m^2	q, Watt	q_a, Watt	q_u, Watt	q_L, Watt	η_o, %
08.0	822.1	1644.2	1189.6	1031.9	157.7	62.76
09.0	865.8	1731.6	1426.1	1164.9	261.2	67.27
10.0	919.3	1838.6	1556.7	1277.2	279.5	69.47
11.0	974.0	1948.0	1661.4	1403.0	258.4	72.02
12.0	993.7	1987.4	1699.3	1450.9	248.4	73.00
13.0	985.8	1971.6	1681.6	1420.2	261.4	72.03
14.0	940.2	1880.4	1592.1	1281.0	311.1	68.12
15.0	882.3	1764.6	1453.3	1103.0	350.3	62.51
16.0	725.3	1450.6	1049.6	763.2	286.4	52.61
Total	8108.5	16217.0	13309.7	10895.3	2414.4	-
Mean	900.9	1801.9	1478.9	1210.6	268.3	66.64

The daily average solar energy available (solar radiation flux incident on the tilted solar collector multiplied by its surface area) during the experimental period was 16.217 kWh (58.381 MJ). There were obvious differences in solar energy available for the days recorded during the drying period. The differences in daily solar energy available can be attributed to the effect of the atmospheric conditions during the experimental period. They were also clear differences in hourly average solar energy available from 8 to 16 h. These obvious differences can be attributed to the variation in solar altitude angle from early morning to late afternoon.

The flat-plate solar collector absorbed various amount of solar energy available because the absorbed solar energy is strongly dependent upon the optical efficiency of the solar collector (τ α). The optical efficiency is commonly affected by solar incident angle which was varied from sunrise to sunset. Therefore, the optical efficiency value increased from sunrise till attained the maximum value at noon and then decreased until reached the minimum value prior to sunset. The daily average absorbed solar energy during the drying period was 13.310 kWh (47.916 MJ), which gave an average optical efficiency of 82.07%. The absorbed solar energy (q_a) was plotted against the solar energy available (q) during the drying period (Fig. 5). Regression analysis revealed a highly significant linear relationship ($r = 0.9261$; $P > 0.001$) between these parameters. The regression equation for the best fit was:

$$q_a = 0.8244\ (q) \qquad (18)$$

This regression analysis also indicated that, the absorbed solar energy could express as:

$$q_a = (\tau\ \alpha)\ (q) \qquad (19)$$

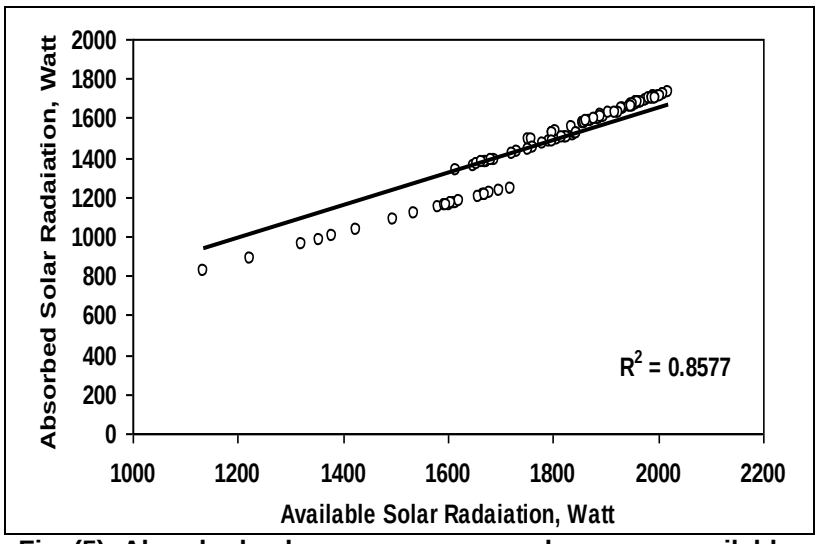

Fig. (5): Absorbed solar energy versus solar energy available.

Regression equation is definitely the numerical expression of the equation (19). The slope of equation is approximately equal to the optical efficiency, which is the product of transmittance (τ) of the glass cover and absorptance (α) of the black absorber plate. Only at and around noon the sun's rays were approximately perpendicular to the solar collector surface that stationary non tracking. Consequently, the optical efficiency of the solar collector was varied from hour to hour and day to another due to variation in the solar incident angles.

The value of heat removal factor (F_R) is equivalent to a conventional heat exchanger effectiveness, which defined as the ratio of the actual heat

transfer to the maximum possible heat transfer. The maximum possible useful heat energy gain (heat transferred) in a solar collector occurs when the completely solar collector temperature is at the inlet fluid temperature; heat losses to the convection environment are then at the minimum level. The heat removal factor of solar collector multiply by this maximum possible useful heat energy gain is equal to the actual useful heat energy gain (q_u). The daily average, heat removal factor during the drying period for mass flow rate of 0.1172 kg/s was 0.8214. The daily average absorbed solar energy converted into useful heat gain depends highly upon the heat removal factor. Heat removal factor depends on three important parameters, the solar collector flow factor, the collector efficiency factor, and the temperatures difference between the operating fluid (air) and the absorber plate. The daily average absorbed solar energy converted into useful heat gain during the test period was 10.895 kWh. Useful heat gain varied from hour to hour and day to another and during the experimental period due to the variations in air inlet temperature (ambient air temperature surrounding the solar collector) and solar energy available. Useful heat gain during the test period was plotted against solar energy available (Fig. 6). Regression analysis revealed a highly significant linear relationship (r = 0.9863; P > 0.001) between these parameters. The regression equation for the best fit was:

$$q_u = 0.6772\ (q) \qquad (20)$$

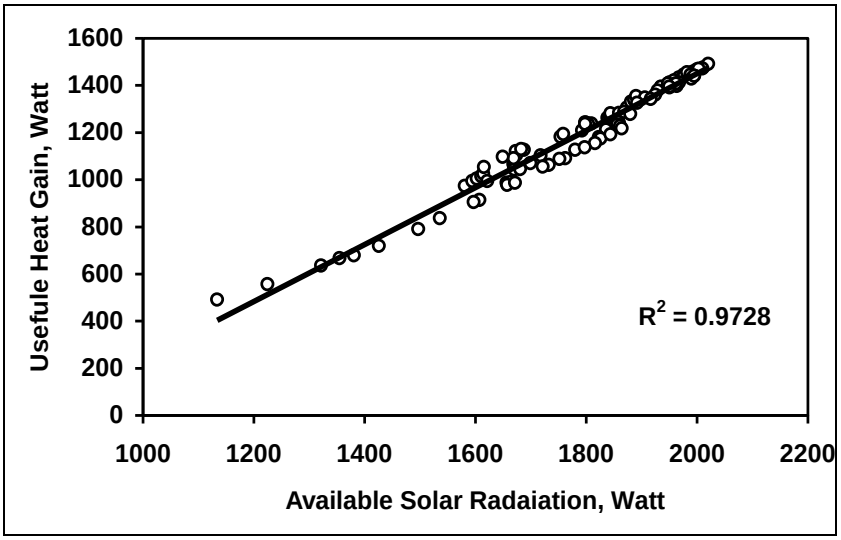

Fig. (6): Useful heat gain to storage versus solar energy available.

The regression analysis also revealed that, the slope of the regression equation is almost equal to the daily average overall thermal efficiency of the solar collector during the test period.

The difference between the absorbed solar energy and the useful heat gain is the actual solar collector heat losses (Duffie and Beckman, 2006). The daily average heat energy lost from the solar collector during the test period

was 2.414 kWh. These data evidently revealed that, the hourly average heat energy losses from the solar collector afternoon (302.3 W) were higher than that before noon (239.2 W). This variation (63.1 W) was due to the inlet air temperatures of the operating fluid (air) during the first four hours (from 8 to 11 h) of each day were lower than that during the last four hours of the day (from 13 to 16 h). The heat losses from solar collectors (q_L), were plotted against the temperature difference between the absorber plates (T_p) and the ambient air (T_a) as shown in Fig. (7). Regression analysis showed a highly significant linear relationship (r = 0.9294; P > 0.001) between these parameters. The regression equation for the best fit was:

$$q_L = 11.004 (T_p - T_{aic}) \quad (21)$$

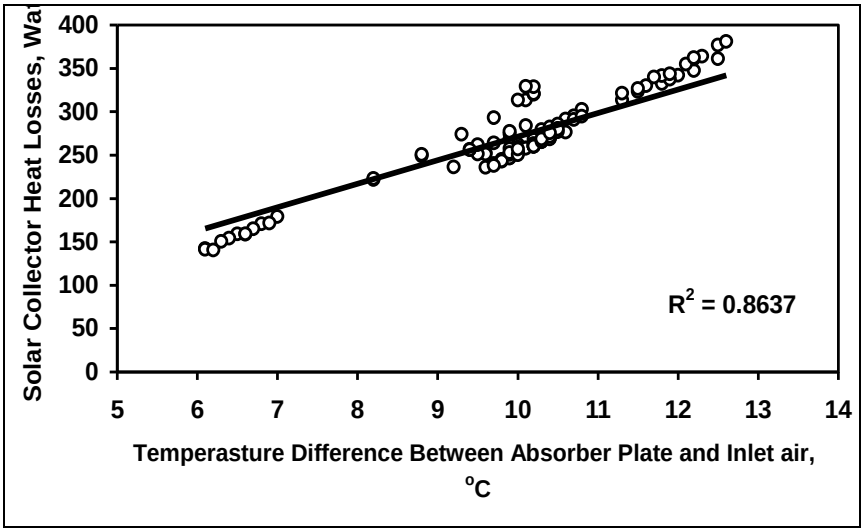

Fig. (7): Solar collector heat losses versus temperature difference between absorber plate and inlet air temperature.

Because of the heat losses are highly dependent upon the overall heat transfer coefficient (U_o) which is a function of temperature difference between the mean absorber plate and ambient air surrounding the solar collector, and wind speed. The regression analysis also showed that, the slope of the regression equation (21) is equal to the product of overall heat transfer coefficient (U_o = 5.502 W/m^2 ºC) and the surface area of the solar collector (A_c = 2 m^2).

The product of optical efficiency and the heat removal factor is the overall thermal efficiency of the solar collectors. Otherwise, the overall thermal efficiency is the ratio of the useful heat energy acquired by the working fluid (air) leaving the solar collector to the solar energy available. The daily averages overall thermal efficiency of the solar collector during the drying period 66.64%, consequently, 33.36% of the solar energy available was lost. To assess the most dominant parameters affecting overall thermal efficiency, the obtained data were examined with the normalized temperature rise D_T). Tests executed with a range of inlet temperature conditions of the

working fluid (air). To minimize effects of heat capacity of the solar collector, tests carried out in nearly symmetrical pairs, one before and one after solar noon as recommended by Duffie and Beckman (2006). The overall thermal efficiencies (η_o) were plotted against the normalized temperature rise (D_T) as shown in Fig. (8). Regression analysis revealed a highly significant linear relationship (r = 0.9714; P > 0.001) between these parameters. The regression equation for the best fit was:

$$\eta_o = 0.6772 - 4.4388\, D_T \times 10^{-2} \quad (22)$$

The regression analysis also revealed that, the solar collectors overall thermal efficiency can be expressed as:

$$\eta_o = \frac{q_c}{q} = F_R(\tau\alpha) - U_o F_R \left[\frac{T_{aoc} - T_{aic}}{R} \right], \% \quad (23)$$

$$\eta_o = F_R(\tau\alpha) - U_o F_R (D_T), \% \quad (24)$$

$$\eta_o = a - U_o F_R (D_T), \% \quad (25)$$

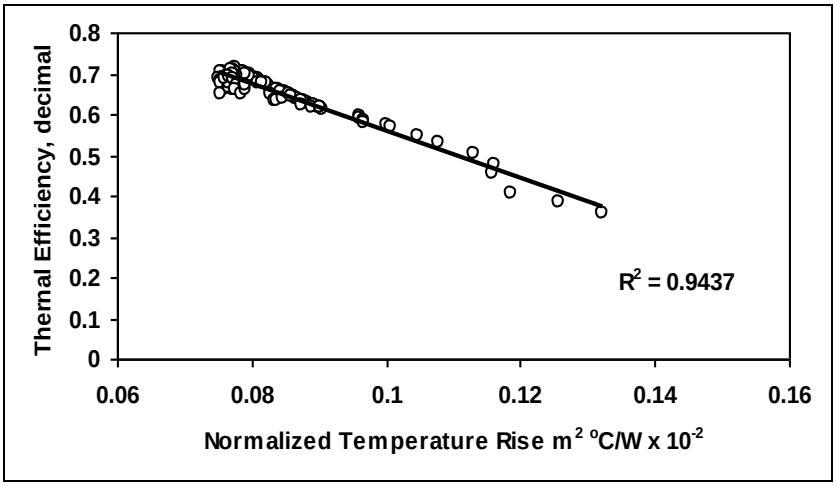

Fig. (8): Overall thermal efficiency versus normalized temperature rise during the drying period.

Regression equation is definitely the numerical expression of Equation (25). The Y-intercept (a) is equal to the product of the heat removal factor (F_R = 0.8214), and optical efficiency (τα = 0.8244). The slope is equal to the product of the heat removal factor (F_R) and overall heat transfer coefficient (U_o = 5.404 W/m^2 ºC). The plot of overall thermal efficiency (η_o) versus normalized temperature rise (D_T) was straight line with Y-intercept F_R (τα) and slope (- F_R U_o). It is clear that U_o is a function of temperatures difference between absorber plate and inlet air entering the solar collector and wind speed. Therefore, the heat removal factor (F_R) during the first four hours (from 8 to 11 h) was 0.8575, while, it was 0.7853 during the last four hours prior to sunset. Moreover, some variations of the relative proportions of; beam, diffuse, and ground reflected components of solar radiation occurred.

For the duration of the test period, the solar collector air heater resulting in raised the ambient air temperature by an average 10.5ºC (from 31.1 to 41.6ºC). The heated air by solar collector was utilized during the drying period by entering it into the solar tunnel drying. Consequently, solar collector air heater was contributed in providing the drying air temperature at desired level (47.2ºC). The thermal performance analysis of solar tunnel dryer depends on the geometric characteristics of dryer, mass flow rate of working fluid (air), and the climatic conditions surrounding the dryer. The climatic conditions were associated with the intensity of solar radiation, ambient air temperature, air relative humidity, and wind speed and its direction. The hourly average solar energy flux incident outside and inside the solar tunnel dryer during the drying period is the sum of two components; beam solar radiation directly incident from the sun and diffuse solar radiation that diffused from the sky and incident on the horizontal plane. The hourly average solar energy flux incident outside and inside the solar tunnel dryer during the experimental period varied from hour to hour and day to another during the test period due to the sky cover (clouds) solar altitude angle, and solar incident angle as shown in Fig. (9). Therefore, the experiments were run only through nine hours (from 7.30 am to 16.30, solar time).

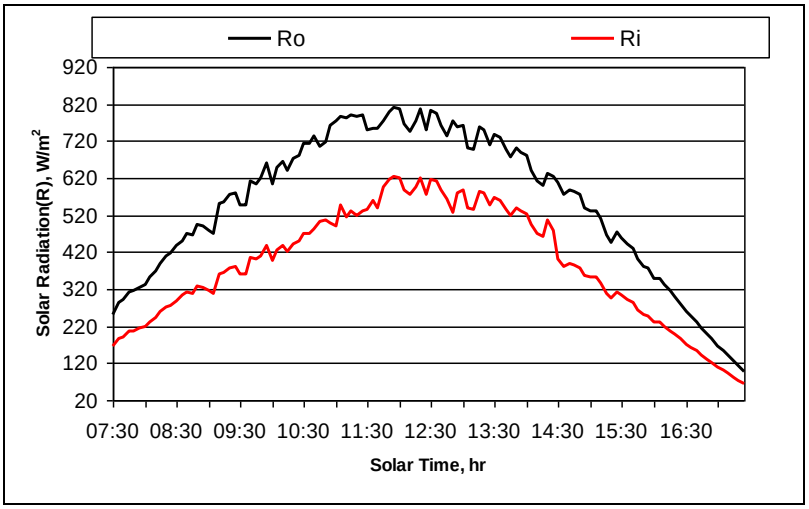

Fig. (9): Hourly average solar radiation flux incident outside (R_o) and inside (R_i) the solar tunnel dryer.

The actual solar radiation recorded inside the solar dryer was lower than that outside because of, the reflectance, absorptance, and transmittance of the dryer covering material (Fiberglass reinforced plastic). The hourly average solar radiation recorded outside and inside the solar dryer, respectively, was 623.0 and 507.8 W/m^2 with cover effective transmittance of 81.85%. To determine the solar radiation penetrating the solar tunnel dryer cover (R_i) as a function of the actual solar radiation flux incident outside (R_o),

all the data recorded during the experimental period were plotted in Fig. (10). Regression analysis revealed a highly significant linear relationship ($r = 0.9961$; $P \leq 0.001$) between these parameters. The regression equation for the best fit under specific conditions was:

$$\mathbf{R_i \text{ (solar dryer)} = 0.8185\ (R_o)} \qquad \mathbf{(26)}$$

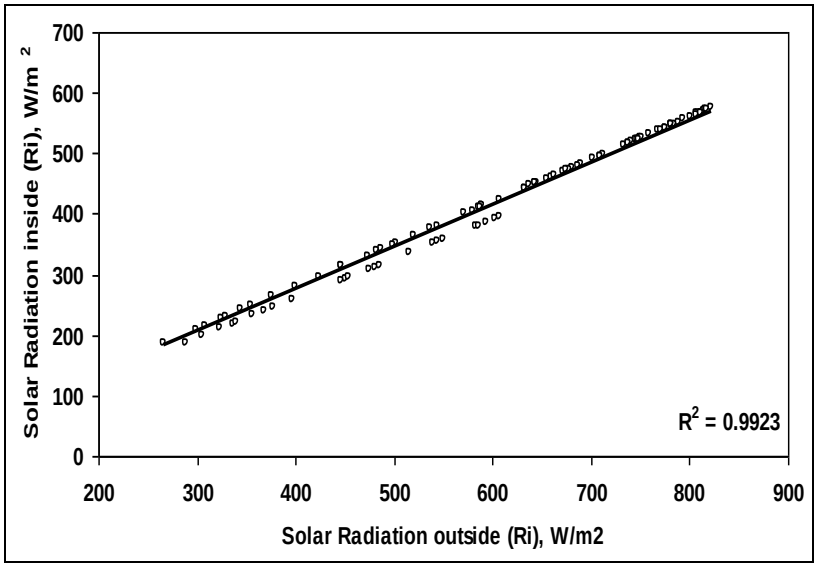

Fig. (10): Solar radiation flux incident inside the solar tunnel dryer versus solar radiation flux incident outside the dryer.

The regression analysis also showed that, the slope of the regression equations is equal to the effective transmittance of the solar tunnel dryer cover during the test period. The effective transmittance of the fiberglass cover varied from hour to another and during the experimental period due to the variation in the solar altitude angle and the solar incident angle. Since, the solar energy available inside the solar dryer is the main source of energy used in the drying process of agricultural products during the daylight-time; it has the main effect on increasing the temperature of drying air which may be considered as a very important parameter affecting drying process. The air temperatures inside the solar dryer (T_{aid}) ranged from 36.5 to 56.0ºC during the test period. The hourly average air temperature just leaving the solar collector air heater, air temperature inside the solar dryer, respectively, was 41.6 and 47.2ºC, while the air temperature outside the dryer was 31.1ºC. Accordingly, the complied data showed that, the solar collector air heater and the solar dryer increased the air temperatures by 10.5 and 16.1°C above the outside air temperature.

The hourly average air temperatures outside, just leaving the solar collector air heater and inside the solar dryer during the drying period are plotted in Fig. (11). It can be observed a variation in air temperatures with solar time. It evidently revealed that, the diurnal variations amplitude under solar collector air heater and solar dryer were more significant. The maximum

air temperature inside the solar tunnel dryer during the test period reached 56.0ºC, which achieved at and around noon. It also revealed that, at nighttime the air temperature inside the solar dryer was almost balanced with the outside air temperature. While, during the daylight the air temperature was usually greater than that outside the solar dryer. The thermal performance test of the solar dryer during the drying period is listed in Table (2). The daily average solar energy available during the test period was 9.141 kWh (32.908 MJ) of which 5.514 kWh (19.850 MJ) was converted into useful heat energy collected. Useful heat energy collected during the test period (Q_u) was plotted against the solar energy available (Q) as shown in Fig. (12). Regression analysis showed a highly significant linear relationship ($r = 0.9723$; $P \leq 0.001$) between these parameters. The regression equation for the best fit under specific conditions was:

$$\mathbf{Q_u\ (STD) = 0.6260\ (Q)} \qquad \mathbf{(27)}$$

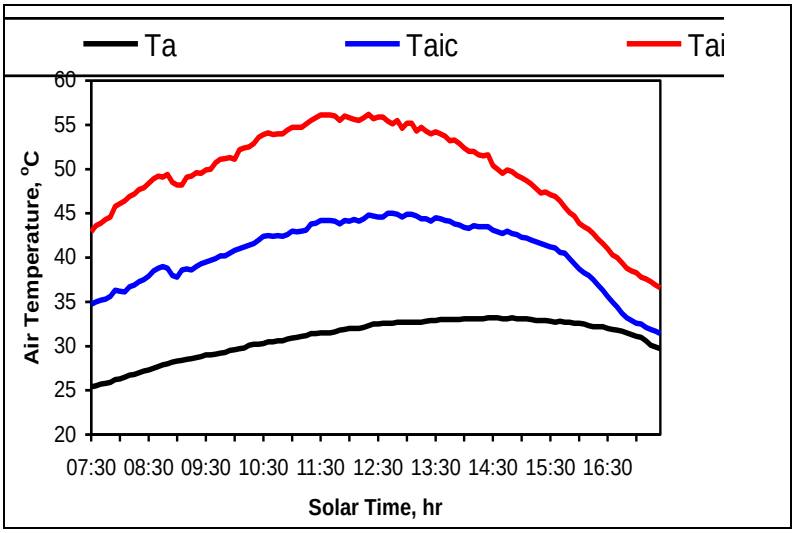

Fig. (11): Air temperatures outside (T_a) and inside the solar dryer (T_{aid}) as a function of drying time.

The regression analysis also showed that, the slope (0.6260) of the regression equation is almost equal to the daily average overall thermal efficiency of the solar tunnel dryer during the drying period.

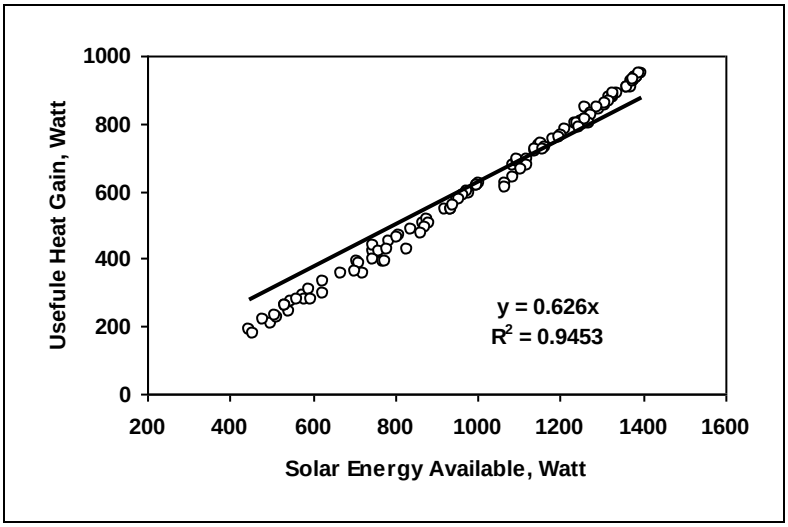

Figure (12): Useful heat gain to storage versus solar energy available.

Table (2): Hourly average solar energy flux incident on the horizontal surface outside (R_o) and inside the solar dryer (R_i), solar energy available (Q) and absorbed solar energy (Q_a), useful heat gain (Q_u), heat energy losses (Q_L), and overall thermal efficiency (η_o) during the drying period.

Solar Time, hr	R_o, W/m^2	R_i, W/m^2	Q, Watt	Q_a, Watt	Q_u, Watt	Q_L, Watt	η_o, %
08.0	397.7	300.7	601.4	391.6	306.4	295.0	50.95
09.0	543.8	430.2	860.4	592.0	498.7	361.7	57.96
10.0	675.0	550.7	1101.4	767.8	690.9	410.5	62.73
11.0	768.4	646.8	1293.6	904.6	848.0	445.6	65.55
12.0	805.8	687.6	1375.2	962.6	922.1	453.1	67.06
13.0	771.3	649.2	1298.4	908.0	847.1	451.3	65.24
14.0	704.3	574.6	1149.2	801.1	707.6	441.6	61.57
15.0	552.8	437.3	874.6	601.8	491.1	383.5	56.15
16.0	388.2	293.5	587.0	382.2	284.7	302.3	48.50
Total	5607.3	4570.6	9141.2	6311.7	5514.4	3544.6	-
Mean	623.0	507.8	1015.7	701.3	612.7	393.8	59.52

The daily average total heat losses from the solar dryer during the drying period were 3.545 kWh (12.762 MJ). The daily average heat energy losses by conduction and convection, and thermal radiation were, respectively, 1.252 kWh (4.507 MJ), 2.057 kWh (7.405 MJ), and 0.236 kWh (0.850 MJ). Consequently, the heat lost due to conduction and convection, air exchange by extracting fan, and thermal radiation, respectively, represented 35.32%, 58.03%, and 6.65% of the total heat losses from the solar tunnel dryer. The daily average overall thermal efficiency of the solar tunnel dryer during the test period was 59.52%, consequently, 40.48% of the solar energy available inside the solar dryer was lost. The overall thermal efficiency varied

from hour to another and during the test period as shown in Table (2). Therefore, the highest overall thermal efficiency (67.06%) was achieved at 12 noon, while, the lowest value (48.50%) occurred before sunset (at 16.00 h).

CONCLUSION

A novel mixed mode solar dryer connected to solar collector air heater was tested and evaluated for thermal performance analysis by operating the system on forced convection. For the duration of this experimental work, the solar energy available was observed as the most important parameter affecting thermal performance of both solar collector air heater and solar tunnel dryer. The useful heat gain, normalized air temperature rise, and overall thermal efficiency were found to be strongly affected by the solar energy available. The daily average solar energy available inside the solar collector air heater and solar tunnel dryer during the experimental period was 16.217 and 9.141 kWh (58.381 and 32.908 MJ) of which 10.895 and 5.514 kWh (39.222 and 19.850 MJ), respectively, converted into useful heat gain. The daily average overall thermal efficiencies of the solar collector air heater and solar dryer, respectively, were 66.64% and 59.52%. Consequently about 33.36% and 40.48% of the solar energy available inside the both systems was lost, respectively.

REFERENCES

Afriyie, J. K.; Nazha, M. A. A.; Rajakaruna, H.; and Forson, F. K. (2009) "Experimental investigations of a chimney-dependent solar crop dryer" Renewable Energy, 34: 217-222.

ASHRAE (2005) "Handbook of Fundamentals" American Society of Heating Refrigerating and Air Conditioning Engineers, New York, USA

Chen, W.; and Qu, M. (2014) "Analysis of the heat transfer and air flow in solar chimney drying system with porous absorber" Renewable Energy, 63: 511-518

Condori, M.; and Saravia, L. (2003) "Analytical model for the performance of the tunnel drier" Renewable Energy, 28: 467-485

Cordeau, S.; and Barrington, S. (2011) "performance of unglazed solar ventilation air pre-heaters for boiler barns" Solar Energy, 85: 1418-1429.

Duffie, J. A.; and Beckman, W. A. (2006) "Solar Engineering of Thermal Processes" New York, N. Y., John Wiley and Sons.

Elkadraoui, A.; Kooli, S.; Hamdi, I.; and Farhat, A. (2015) "Experimental investigation and economic evaluation of a new mixed-mode solar greenhouse dryer for drying red pepper and grape" Renewable Energy, 77: 1-8

El-khawajah, M. F.; Aldabbagh, L. B. Y.; Egelioglu, F. (2011) "The effect of using transverse fins on a double pass flow solar air heater using wire mesh as an absorber" Solar Energy, 38: 1479-1487

Goel, V.; and Vashishtha, S. (2010) "thermal performance optimization of a flat platen solar air heater using genetic algorithm" Applied Energy, 87: 1793-1799

Kalogirou, S. M. (2004) "Solar thermal collectors and application" Progress in Energy and Combustion Science, 30: 231–295.

Kumar, A.; Saini, R. P.; Sainin, J. S. (2014) "A review of thermo-hydraulic performance of artificially roughened solar air heaters" Renew Sustain Energy Rev., 37: 100-122.

Lin, W.; Gao, W.; and Liu, T. (2006) "A parametric study on the thermal performance of cross-corrugated solar air collectors" Applied Thermal Engineering, 26:1043-1053.

Mitta, M. K.; Varshney, L. (2006) "Optimal thermo-hydraulic performance of a wire mesh packed solar air heater" Solar Energy, 80: 1112–1120.

Nowzari, R.; Mirzaei, N.; and Aldabbagh, L. B. Y. (2015) "Finding the best configuration for a solar air heater by design and analysis of experiment" Energy Conversion and Management, 100: 131-137.

Sukhatme, S. P.; and Nayak, J. K. (2008) "Solar energy principles of thermal collection and storage" third ed. New Delhi: TMH Publishing Company Limited.

Tian, J.; Kim, T.; Lu, T. J.; Hodson, H. P.; Queheillalt, D. T.; and Sypeck, D. J. (2004) "The effects of topology upon fluid-flow and heat-transfer within cellular copper structures" International Journal of Heat Mass Transfer, 47: 3171-3186

Yeh, J. M.; Ho, C. D.; Lin, C. Y. (2000) "Effect of collector aspect ratio on the collector efficiency of upward type baffled solar air heater" Energy conversions Management, 41: 971-981.

تحليل الأداء الحرارى لسخان الهواء الشمسى المساعد للمجفف النفق الشمسى

صلاح مصطفى عبد اللطيف ، ياسر مختار صالح الحديدى و إيمان محمد يونس محمد

قسم الهندسة الزراعية - كلية الزراعة - جامعة المنصورة

يتناول البحث إجراء تجارب عملية بهدف تحليل الأداء الحرارى لسخان هواء شمسى متصل مع مجفف شمسى على شكل نفق تعمل بنظام الحمل الجبرى يمكن إستخدامهما فى تجفيف المحاصل الزراعية خاصة محصول العنب البناتى. تم إجراء التجارب فوق سطح قسم الهندسة الزراعية بكلية الزراعة جامعة المنصورة (خط عرض 31.045ºN وخط طول 31.37ºE) فى الفترة من ٢٩ أغسطس وحتى ٣ سبتمبر عام ٢٠١٥.

أوضحت النتائج المتحصل عليها أن كمية الطاقة الشمسية المتاحة داخل سخان الهواء الشمسى وداخل المجفف الشمسى النفقى هى أهم عامل مؤثر على الأداء الحرارى لكلا النظامين حيث تأثر كلاً من الطاقة الحرارية المكتسبة والمستفاد بها فى رفع درجة حرارة الهواء ومقدار الزيادة فى درجة الحرارة والكفاءة الحرارية الكلية بالطاقة الشمسية المتاحة. المتوسط اليومى للطاقة الشمسية المتاحة داخل سخان الهواء الشمسى وداخل المجفف الشمسى كانت على التوالى (58.381 and 32.908 MJ)16.217 and 9.141 kWh والتى منها تم تحويل(39.222 and 19.850 MJ) 10.895 and 5.514 kWh إلى طاقة حرارية مكتسبة. بلغت الكفاءة الحرارية الكلية لسخان الهواء الشمسى والمجفف الشمسى على التوالى 66.64% and 59.52% بالتالى فإن حوالى 33.36% and 40.48% من كمية الطاقة الشمسية المتاحة داخل سخان الهواء الشمسى وداخل المجفف الشمسى النفقى قد تم فقدها على التوالى.